PHYSICAL REVIEW A VOLUME 47, NUMBER 5 MAY 1993

Cross section for coincident two-photon emission at ±90° in electron-atom collisions

Jingai Liu and C. A. Quarles
Texas Christian University, Fort Worth, Texas 76129
(Received 10 September 1992; revised manuscript received 14 December 1992)

The cross section for coincident two-photon emission in the bombardment of thin targets of Al, Cu, Tb, and Au with 70-keV electrons has been measured in the ±90° geometry. The present results for Au are about two orders of magnitude lower than the results of Altman and Quarles [Phys. Rev. A **31**, 2744 (1985); Nucl. Instrum. Methods Phys. Res. A **240**, 538 (1985)] for 75-keV incident electrons in the same geometry. The present results are generally consistent with the relativistic first Born approximation for double bremsstrahlung. While an explanation for the larger yield observed earlier is still not available, we believe that the increased sensitivity of the present coincidence setup makes the present data more reliable. We have also directly observed a coincident cross-talk effect due to the escape of a Ge K x ray from one detector and its coincident detection by the second detector. This effect leads to a large coincidence yield when an energy window includes the Ge K x ray. The implication of such escape effects in ±90° geometry experiments is discussed.

PACS number(s): 34.80.Dp, 79.20.Kz

I. INTRODUCTION

The first data on coincident two-photon emission in electron-atom interactions were reported in 1985 by Altman and Quarles [1]. A 75-keV electron beam was used to bombard thin targets (about 50 μg/cm^2) of Ag, Tb, Au, and U; and the two photon detectors were placed at ±90° to the incident beam to detect the two-photon emission. The results were interpreted as double bremsstrahlung and were about two orders of magnitude larger than the theory calculated by integrating the relativistic first Born approximation formula of Smirnov [2].

The significant discrepancy has stimulated additional theoretical and experimental work. The cross section was computed in the nonrelativistic Coulomb approximation by Veniard, Maquet, and Gavrila [3] and by Florescu and Djamo [4], and, while different in detail, was found to be of about the same order of magnitude as the relativistic result. After consideration of a variety of possible experimental background processes that could lead to two-photon emission, it was suggested that the data of Ref. [1] could be largely due to the cross-talk effect of double bremsstrahlung in the detector windows produced by electrons elastically scattered in the target [5]. Recent direct measurement of the double bremsstrahlung in thick targets [6], however, has shown that this effect is not large enough to explain the discrepancy of Ref. [1]. The recent measurements [7] of two-photon emission in a ±45° geometry have found much better agreement with the relativistic theory. However, while the order of magnitude of the ±45° data agrees with theory, there is a deviation from the Z^2 dependence predicted by the first Born approximation. The data in the 45° geometry were taken with a coincidence electronics system that was much more sensitive than that used in Ref. [1]. Thus it was decided to remeasure the two-photon emission cross section in the ±90° geometry. The present experiment, while a repeat of the experimental geometry of Ref. [1], uses different detectors and a different scattering chamber, designed to reduce some of the background effects considered significant in Ref. [1]. Thus the data reported here, while for 70 keV instead of 75 keV incident electrons, are intended to replace the data of Ref. [1].

In the special case when one of the energy windows includes the Ge K x-ray energy, the measured two-photon cross section is two orders of magnitude larger than the double bremsstrahlung theory. This arises from the cross-talk effect that occurs in the ±90° geometry due to the escape of the Ge K x ray from one detector and the coincident detection of that x ray in the other detector. This rate can be explained in terms of the tabulated single bremsstrahlung theoretical cross sections [8], and a Ge K x-ray escape probability of several percent. The implication of this type of cross-talk escape effect for other experiments in the ±90° geometry will be discussed.

II. TIME COINCIDENT MEASUREMENT

The target chamber is shown to scale in Fig. 1. The electron beam is produced by a Cockcroft-Walton linear accelerator. The beam is collimated and strikes a target that is a thin film on a 15-μg/cm^2 carbon backing mounted on an aluminum target frame within the target chamber. The chamber is electrically isolated and serves as a Faraday cup to collect the total charge. The detectors are 100-mm^2 area, 10-mm-thick high-purity (HP) planar Ge detectors. They view the target at 90° through a 10-mil Mylar window that serves (1) to electrically isolate the detector housing from the target chamber, (2) as a vacuum window, and (3) to absorb elastically scattered electrons. The collimators are placed to define the solid angle, to reduce the photon background from electrons that strike the chamber walls, and to restrict cross talk between the detectors mainly to those photons that pass from one detector to the other through the target. Not

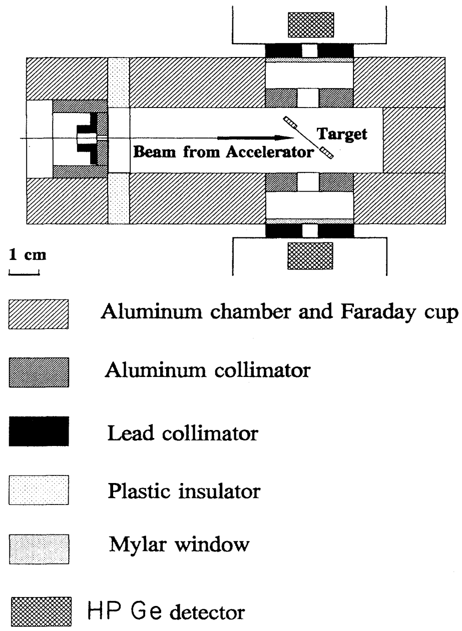

FIG. 1. Scale drawing of the target chamber for the detectors in the 90° geometry.

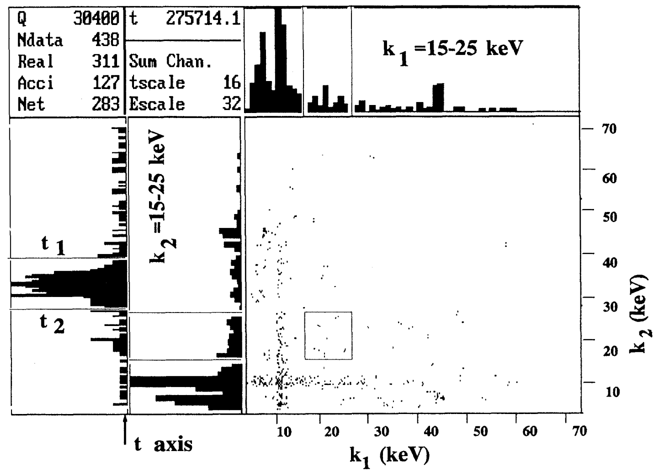

FIG. 2. A portion of the computer screen of the data analysis program showing the coincident time spectrum vertically on the left, single-photon-energy spectra for k_1 and k_2 running horizontally and vertically, and the two-dimensional energy array of net events (reals less the scaled accidentals). This spectrum is for 70-keV electrons on a Tb target. The square box selects an energy window for k_1 and k_2 from 15 to 25 keV, indicated by the cursors in the singles spectra for events defined as real coincidences within a time range t_1 to t_2 indicated by the time cursors. In addition, one can see bands that are due to the Ge K x-ray escape effect and a small cluster of events corresponding to Tb K-L x-ray cascade coincidences at 44 and 7 keV.

shown in the figure is a pump-out port and the port through which the target is introduced. The output of each Hp Ge detector is processed by NIM and CAMAC electronics, which has been previously described [6,9]. The data are collected as events that consist of the energy of each photon and the time between them.

Figure 2 shows a part of the computer screen produced by the data analysis program. The data in Fig. 2 are for a single run for 70-keV electrons on a Tb target. The two-dimensional energy array is the net two-photon coincidence energy spectrum obtained as described below. Also shown are a time spectrum for the events (running vertically on the left side) and two single-photon energy spectra (the top horizontal spectrum and the second vertical spectrum on the left). Several features are evident in the figure. First, there are peaks in the single-photon-energy spectra due to the Tb L x rays at about 7 keV and the Tb K x ray at about 44 keV. A cluster of coincidence events between the Tb K and L x rays can be identified in the two-dimensional spectrum. This Tb K-L cascade coincidence rate has been used previously to calibrate the cross-section scale of the experiment [7]. An additional large sharp peak at the photon energy of 10 keV can also be seen in each single-photon-energy spectrum and as a band in the two-dimensional energy spectrum. This is the escape Ge K x-ray effect discussed in Sec. IV below.

In the time spectrum, the region between the cursors marked t_1 and t_2 indicates the region of the time spectrum defined as containing real coincidences. In this example, the large "real" coincidence peak is due to the events in the Ge escape region of the coincidence spectrum (the bands). To either side of the real region is a background region of accidental counts that are due to incoherent interactions that accidentally produce two photons. The events in the two-dimensional energy array represent the *net* number of real coincidences. This spectrum is built from the events by first constructing a spectrum of those events whose times fall within the interval t_1 to t_2. Then, an accidental event spectrum is formed from those events whose times fall outside the t_1 and t_2 region. The net spectrum shown is computed by subtracting channel by channel the accidental spectrum, properly scaled by the ratio of the real to accidental time intervals, from the real spectrum. The spectrum shown is a four-channel sum of the events, so it represents a coarser resolution spectrum than that available from the data. The statistical error is found in the usual way from the statistical errors in the number of real and accidental events within a particular photon-energy window.

For the computation of a cross section, a "box" or photon-energy window is defined, and a typical case is illustrated in Fig. 2, centered approximately at photon energies of 20 keV with a width of 10 keV. In some cases, such as low real count rate or high accidental count rate, one obtains a negative value for net counts. For clarity in Fig. 2, channels in which the net counts were negative are not plotted. Since the double bremsstrahlung cross sections are very small, long run times and repeated runs are necessary to obtain reasonable statistics, and yet the statistical errors remain the dominant error in the experiment.

III. DOUBLE BREMSSTRAHLUNG CROSS SECTIONS AT ±90° FOR 70-keV ELECTRONS

The experimental value of the double bremsstrahlung cross section can be calculated from

$$\frac{d^4\sigma}{dk_1 dk_2 d\Omega_1 d\Omega_2} = \frac{N_{\text{net}}}{N_e \tau \Delta k_1 \Delta\Omega_1 \varepsilon_1(k_1) \Delta k_2 \Delta\Omega_2 \varepsilon_2(k_2)} . \quad (1)$$

Here, N_e is the number of incident electrons, N_{net} is the net number of coincident counts within the energy window Δk_1 and Δk_2, τ is the target thickness, and $\Delta\Omega$ and ε are the solid angle and efficiency of the indicated detector. In this experiment, the product of solid angle and efficiency of the detectors was measured by using the coincident spectrum of a calibrated ^{133}Ba radioactive source. The targets were Au, Tb, Cu, and Al with thicknesses of 30–50 μg/cm^2 determined within a 20% error. These thicknesses are thin enough for single-collision conditions to apply.

The experimental cross sections for Cu, Tb, and Au are plotted in Fig. 3 and compared to the theory. The cross sections have been scaled by $1/Z^2$ for one photon energy k_1 fixed at 20 keV versus the second photon energy. The photon-energy window widths Δk were both ± 5 keV. The theoretical cross section, shown as the solid line, was calculated by integrating the relativistic first Born approximation formula of Smirnov [2] over the unobserved scattered electron and is corrected by the Elwert factor. As can be seen, the data are consistent with the theory. The errors shown are at the one standard deviation level. In addition to the statistical error shown, there is an additional systematic scale error of $\pm 3\times 10^{-4}$ μb/keV^2 sr^2 due to the choice of the starting channel for the selected energy windows. While the present data generally agree with the theory within the statistical errors, the points for Tb and Au at $k_2 = 50$ keV both appear systematically higher than the theory. In Ref. [1], a similar increase in the cross section for the highest k_2 was observed, and there it was possible that there was some increase due to Compton backscattering. That explanation is not kinematically allowed, however, in the present case. Perhaps, the Born approximation under predicts the cross section near the kinematic end point, as it does in single bremsstrahlung. Considering the systematic and statistical errors, we do not attach any particular significance to the negative values of the Cu cross sections shown in Fig. 3. For each target the results represent a weighted average of at least six runs. The runs were taken with different beam rates, accidental rates, and some with the energy discriminators set to exclude the Ge escape peak. For Cu, the weighted average for each k_2 was negative. Taking the two standard deviation levels as an upper limit, the scaled Cu cross section is less than about 4×10^{-4} μb/keV^2 sr^2.

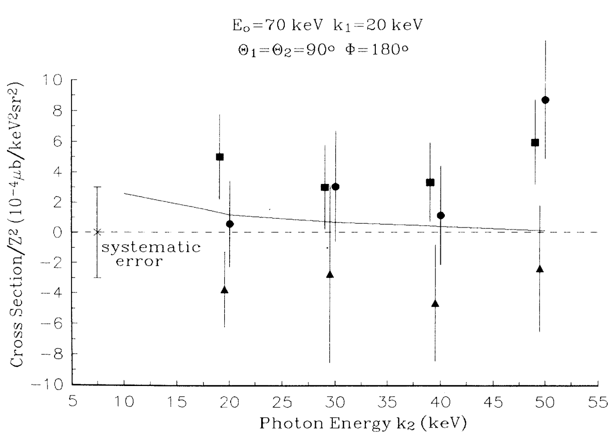

FIG. 3. The cross section for double bremsstrahlung scaled by Z^{-2} vs photon energy of one photon. The second photon is fixed at an energy of 20 keV. The circles are Au, the squares are Tb, and the triangles are Cu. The solid line is the integration of the Smirnov formula with the Elwert factor included. The errors shown are at the one standard deviation level. In addition there is a systematic scale error of $\pm 3\times 10^{-4}$ μb/keV^2 sr^2.

Even though the statistical errors are large, the experiment is able to set an upper limit on the theoretical scaled cross section of about 20×10^{-4} μb/keV^2 sr^2 at the two standard deviation levels. This is further illustrated in Fig. 4 in a semilog plot that shows a comparison of the present results for the differential cross section for Au with the results of Ref. [1]. The open circles are the data of Ref. [1], and the solid circles are the same as those shown in Fig. 3, but here we have also included the point at $k_2 = 10$ keV. As discussed below, this 10-keV point is due to the Ge K x-ray escape effect and not to double bremsstrahlung. The solid line is the same theory shown in Fig. 3. In the photon-energy range of 20–50 keV, the present results are more than an order of magnitude lower than the results of Ref. [1]. Although there is a 5-keV difference in incident energy between the two experiments, and resonance effects in bremsstrahlung production due to polarization bremsstrahlung have been discussed [10], we do not believe that such resonance effects have anything to do with the difference between the present data and those of Ref. [1]. Rather, the present data verify that the results of Ref. [1] had a large background, the exact nature of which still remains unknown, and should not be interpreted as due primarily to double bremsstrahlung.

Figure 5 shows the Z dependence of the double bremsstrahlung cross section. Here, the two photon energies were chosen at 25 keV for each target, and the window width was doubled to ± 10 keV in order to reduce the statistical error. In contrast with the results of the $\pm 45°$ ex-

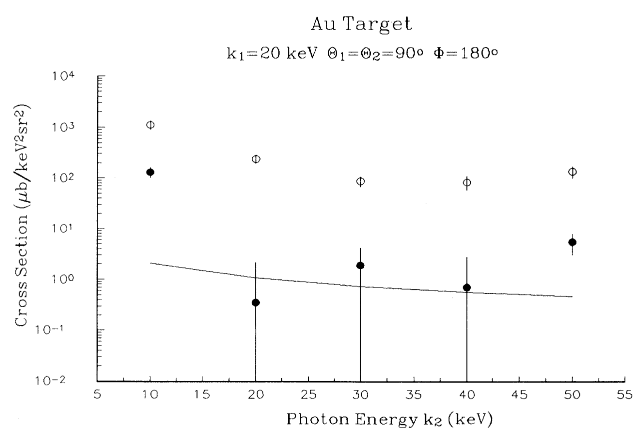

FIG. 4. Comparison of the data of the present experiment (solid circles) with that of Ref. [1] (open circles) for a Au target. Also shown is a point for k_2 at 10 keV, which is due to the Ge K x-ray escape effect and not to double bremsstrahlung. The solid line is from the same theory as in Fig. 3.

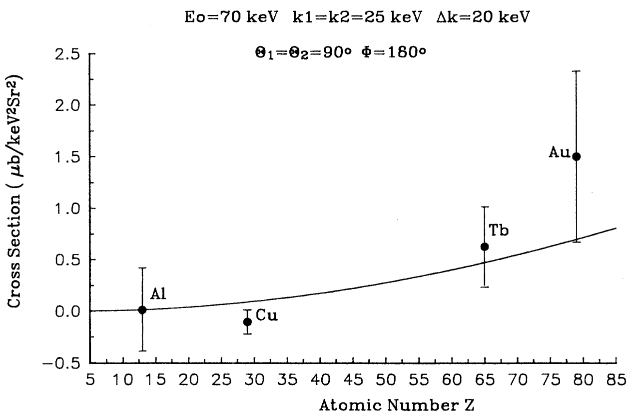

FIG. 5. Z dependence of the double bremsstrahlung cross section for both photons at 25±10 keV. The solid line is from the same theory as in Fig. 3.

periment [7], the present data seem to be consistent with the Z^2 dependence expected from the first Born approximation.

IV. Ge-K X-RAY ESCAPE EFFECT

When the photon-energy range includes the Ge K x-ray energy at 10.1 keV, the cross-talk effect between the two detectors in the ±90° geometry significantly enhances the two-photon yield. The process is as follows: a single photon is produced in the target by single bremsstrahlung. The photon strikes one Ge detector. If the energy is greater than the K-shell binding energy of Ge, the photon may photoionize the K shell, producing a Ge K x ray and a photoelectron. Assume that the photoelectron is detected in the detector but that the Ge K x ray escapes. The Ge K x ray could be detected in coincidence in the second detector that is positioned directly opposite the first.

We have measured the coincident two-photon yields in the Ge K x-ray energy range. The escape x ray at 10 keV forms a narrow coincidence band in the two-dimensional energy spectrum (see Fig. 2). If a window including the Ge K x-ray energy is chosen at 10±1 keV, and the continuum energy window is 25±10 keV, the experimental two-photon yield can be calculated from tabulated single bremsstrahlung cross sections [8] and the known geometry. We obtain an estimated Ge K x-ray escape probability for the targets of Au, Tb, and Cu of 3.6%, 3.2%, and 3.8%, respectively. This is consistent with what is expected for the planar Ge detector used in the experiment.

The observation of the escape effect has implications for other experiments in the ±90° geometry. A recent measurement of two-photon coincidences from 8–15-keV electrons on Ar, Kr, and Xe gas targets in the ±90° geometry has reported a significant enhancement of the rate over the nonrelativistic double bremsstrahlung theory [11]. The detectors used were a Si(Li) solid-state detector and an argon proportional counter. Some escape effect is expected to occur for energy windows around 3 and 1.7 keV from either Ar or Si K x rays. It does not appear from considerations of the geometry that in this case the escape effect is sufficient to explain the entire measured rate [12]. It does appear plausible, however, that the Ar K x-ray escape effect is the origin of the enhancement of Xe data by a factor of about 4 over that of Ar or Kr. This can be understood as due to the addition of Xe K x rays as well as bremsstrahlung from the target gas when compared to Ar or Kr. The Xe K x rays have just the right energy after escape of the Ar K x ray to trigger the coincident energy channel in which the enhancement is observed.

V. CONCLUSIONS

The remeasurement of the double bremsstrahlung cross section in the ±90° geometry has obtained results that are about two orders of magnitude lower than previous results and in better agreement with the relativistic first Born approximation theory. While it was not the purpose of this work to explain the much higher rate observed earlier, the increased sensitivity of the present coincidence electronics system definitely rules out such a large yield as due to double bremsstrahlung and insures that the present data are more reliable. Thus we intend that the present data should replace the data of Ref. [1].

An enhancement of the two-photon rate when one of the photon-energy windows includes the Ge K x-ray energy is caused by the x-ray escape effect that is clearly seen in the present experiment. The Ge K x-ray escape probability for the geometry of the present experiment was measured to be about 4%, which is consistent with what may be expected for the planar Ge detectors used.

ACKNOWLEDGMENTS

Support of this research by the Welch Foundation and the TCU Research Fund is gratefully acknowledged. We also appreciate the help of Darren Kahler.

[1] J. C. Altman and C. A. Quarles, Phys. Rev. A **31**, 2744 (1985); Nucl. Instrum. Methods Phys. Res. A **240**, 538 (1985).

[2] A. I. Smirnov, Yad. Fiz. **25**, 1030 (1977) [Sov. J. Nucl. Phys. **25**, 548 (1977)].

[3] V. Veniard, A. Maquet, and M. Gavrila, Phys. Rev. A **35**, 448 (1987).

[4] V. Florescu and V. Djamo, Phys. Lett. A **119**, 73 (1986).

[5] H. E. Lehtihet and C. A. Quarles, Phys. Rev. A **39**, 4274 (1989); Nucl. Instrum. Methods. Phys. Res. A **280**, 202 (1989).

[6] Jingai Liu, D. L. Kahler, and C. A. Quarles, Phys. Rev. A (to be published).

[7] D. L. Kahler, J. Liu, and C. A. Quarles, Phys. Rev. Lett. **68**, 1690 (1992).

[8] L. Kissel, C. A. Quarles, and R. H. Pratt, Atom. Data Nucl. Data Tables **28**, 381 (1983).

[9] C. A. Quarles, D. Kahler, H. E. Lehtihet, and D. Lawrence, Nucl. Instrum. Methods Phys. Res. B **56/57**, 184 (1991).

[10] D. L. Kahler, Jingai Liu, and C. A. Quarles, Phys. Rev. A **45**, R7663 (1992).

[11] R. Hippler, Phys. Rev. Lett. **66**, 2197 (1991).

[12] R. Hippler (private communication).